Poly(vinyl alcohol)–Polyacrylamide Blends with Cesium Salts of Heteropolyacid as a Polymer Electrolyte for Direct Methanol Fuel Cell Applications

M. Helen,[1] B. Viswanathan,[1] S. Srinivasa Murthy[2]

[1]*National Centre for Catalysis Research, Department of Chemistry, Indian Institute of Technology Madras, Chennai 600 036, India*
[2]*Department of Mechanical Engineering, Indian Institute of Technology Madras, Chennai 600 036, India*

Received 9 July 2009; accepted 26 November 2009
DOI 10.1002/app.31940
Published online 22 February 2010 in Wiley InterScience (www.interscience.wiley.com).

ABSTRACT: A class of inorganic–organic hybrid membranes with low methanol permeability characteristics for possible direct methanol fuel cell (DMFC) applications was architected, formulated, and fabricated through the blending of poly(vinyl alcohol) (PVA) and polyacrylamide (PAM) followed by crosslinking with glutaraldehyde (Glu). Cesium salts of different heteropolyacids, including phosphomolybdic acid (PMA), phosphotungstic acid (PWA), and silicotungstic acid (SWA), were incorporated into the polymer network to form corresponding hybrid membrane materials, namely, PVA–PAM–CsPMA–Glu, PVA–PAM–CsPWA–Glu, and PVA–PAM–CsSWA–Glu, respectively (where "Cs" together with a heteropolyacid abbreviation indicates the cesium salt of that acid). All the three hybrid polymer membranes fabricated exhibited excellent swelling, thermal, oxidative, and additive stability properties with desired proton conductivities in the range 10^{-2} S/cm at 50% relative humidity. A dense network formation was achieved through the blending of PVA and PAM and by crosslinking with Glu, which led to an order of magnitude decrease in the methanol permeability compared to the state-of-the-art commercial Nafion 115 membrane. The hybrid membrane containing CsSWA exhibited a very low methanol permeability (1.4×10^{-8} cm^2/s) compared to other membranes containing cesium salt of heteropolyacids such as PMA and PWA. The feasibility of these hybrid membranes as proton-conducting electrolytes in DMFC was investigated, and the preliminary results were compared with those of Nafion 115. The results illustrate the attractive features and suitability of the fabricated hybrid membranes as an electrolyte for DMFC applications. © 2010 Wiley Periodicals, Inc. J Appl Polym Sci 116: 3437–3447, 2010

Key words: crosslinking; membranes; blends

INTRODUCTION

Direct methanol fuel cell (DMFC) technology is considered an alternative energy source for portable applications because of the DMFCs' high energy density, low-temperature operation, and system simplicity and the ease of handling liquid fuel methanol.[1] A reliable and successful performance of DMFC depends critically on the role played by the membrane, one of the main components of a fuel cell. Hence, membranes having a high proton conductivity, low methanol permeability, and good electrochemical and dimensional stability have always been targets for DMFC application. Extensive efforts have been made to reduce the methanol permeability in the polymer electrolyte membranes through various approaches,[2] for example, (1) reduction of the proton transport channels by the incorporation of various ceramic fillers,[3,4] crosslinking,[5–10] or the use of different block copolymers[11–13]; (2) modification of the surface of the membrane by the application of plasma, ion, or electron beams, which thereby affects the transport properties of the membrane;[14–17] or (3) the design of inorganic–organic hybrid membranes.[18–23] The later approach has attracted attention because such hybrids may show controllable thermal and mechanical properties by virtue of the combination of the properties of organic polymers and inorganic compounds, such as hygroscopic oxides or solid inorganic proton conductors.

Among various hydrophilic polymers, poly(vinyl alcohol) (PVA) exhibits desired characteristics, such as enhanced chemical stability, and it acts as an excellent methanol barrier[24] and has a film-forming capacity, which is essential for an ion-exchange membrane. Since 1986,[25] a number of research groups have investigated PVA-based proton conducting membranes.[22,23,26–29] PVA membranes with appropriate swelling properties and good proton conductivities are needed for use in fuel cells.[22,23,26] Increasing the water content in the membranes

Correspondence to: B. Viswanathan (bvnathan@iitm.ac.in).

would result in a loss of dimensional stability and cause an increase in methanol permeability. Polymer swelling can be reduced by blending, crosslinking, or copolymerization with other suitable polymers, whereas proton conductivity can be increased by the formation of hybrids by the incorporation of proton conductors such as heteropolyacids.[23,24,26,30–33] A major limiting factor in the use of heteropolyacids as membrane materials for fuel cell application is their extreme solubility in aqueous media. This difficulty can be surmounted by the formation of hybrids with cesium salts of heteropolyacids.[22,23,34]

In this article, we report on the formulation and fabrication of a new class of hybrid membranes containing cesium salts of different heteropolyacids, including phosphomolybdic acid (PMA), phosphotungstic acid (PWA), and silicotungstic acid (SWA), incorporated into a PVA–polyacrylamide (PAM) blend. For the first time, a PVA–PAM polymer matrix was proposed and chosen by us to formulate hybrid membrane materials with salts of heteropolyacids. A simple fabrication route was adopted for the preparation of these hybrid materials. These membranes were characterized through various physicochemical techniques, morphological studies, and permeability experiments. The suitability of these membranes for DMFC application was explored through careful investigation of various required key characteristics of the membrane, including proton conductivity, water uptake, and ion-exchange property. The membranes exhibited the desired properties for DMFC application, including low methanol crossover, optimum swelling with desired proton conductivity, and excellent additive and oxidative stability with the additional advantage of cost effectiveness compared to current commercial Nafion membranes.

EXPERIMENTAL

Membrane fabrication

Cesium salts of various heteropolyacids, including PMA, PWA, and SWA, were synthesized at room temperature (RT) by the neutralization of respective acid solution with an appropriate amount of 0.1*M* cesium carbonate solution. We attempted to control the number of protons substituted to two by controlling the stoichiometry of the added cesium carbonate solution. The white precipitate obtained was dried at RT and kept under the constant humidity of air until a constant mass was attained.

The hybrid membranes were fabricated through a solution-cast method. A 10.0 wt % solution of PVA (molecular weight = 125,000; SRL Chemicals, Mumbai, India) solution in water was prepared under vigorous stirring at 70°C. To this solution, a mixture of 10.0 wt % PAM (molecular weight = 5,000,000, Otto Kemi, Mumbai, India) dissolved in water and a required quantity of one of the cesium salts of the heteropolyacids (i.e., PMA, PWA, or SWA) were added and stirred for 6 h to obtain a homogeneous solution. The weight percentage of PAM and heteropolyacid in the hybrid membrane was maintained as 10.0 wt % each. The homogeneous solution was spread uniformly on a clean glass plate and leveled perfectly. We slowly removed water by keeping the glass plate at RT, and the dried membrane was detached from the glass plate.

The obtained dry membrane was immersed in the crosslinking bath containing glutaraldehyde (Glu; 25 wt % Glu solution in water, SRL Chemicals, Mumbai, India), acetone, and hydrochloric acid for 30 min at RT [75% (v/v) aqueous–acetone mixture containing 2 mL of Glu and 2 mL of concentrated HCl]. The crosslinking time was optimized as 30 min for the concentration of Glu taken. After the completion of crosslinking, the membrane was removed from the crosslinking bath, washed repeatedly with deionized water, and dried at ambient temperature (Scheme 1).

Membrane characterization

The Fourier transform infrared (FTIR) spectroscopic measurements (Nicolet 6700 FTIR instrument interfaced with Omnic software; Thermo Scientific, Waltham, MA) for the hybrid membranes were made in the wave-number range 600–4000 cm^{-1} at RT. X-ray diffraction (XRD) patterns were collected with a Rigaku D/max 2400 powder diffractometer (Tokyo, Japan) with Cu Kα radiation. Thermogravimetric analysis (TGA) was performed on a PerkinElmer Diamond (Wellesley, MA) thermogravimetry/differential thermal analysis instrument at a heating rate of 20 K/min under an air atmosphere. Morphological characteristics of the hybrid membrane materials were examined with scanning electron microscopy (SEM; Quanta 200, FEI; Hillsboro, OR) so that we could observe the microstructures. All of the images were taken in secondary electron mode. We tested the oxidative stability of the fabricated membranes by immersing the membrane sample (90–100 mg) in 50 mL of Fenton's reagent (3% H_2O_2 containing 2 ppm $FeSO_4$) at RT. The membrane samples were intermittently taken out of the oxidative solution and weighed after the surface-attached water was removed. The oxidative stability of the fabricated hybrid membranes was evaluated from the weight change of the membrane stripe. Proton conductivity studies of the fabricated membranes were done with an alternating-current impedance technique (PARSTAT 2263, Oak Ridge, TN) with a four-electrode probe method, in which the alternating-current frequency was scanned from 1 MHz to 1 Hz at a

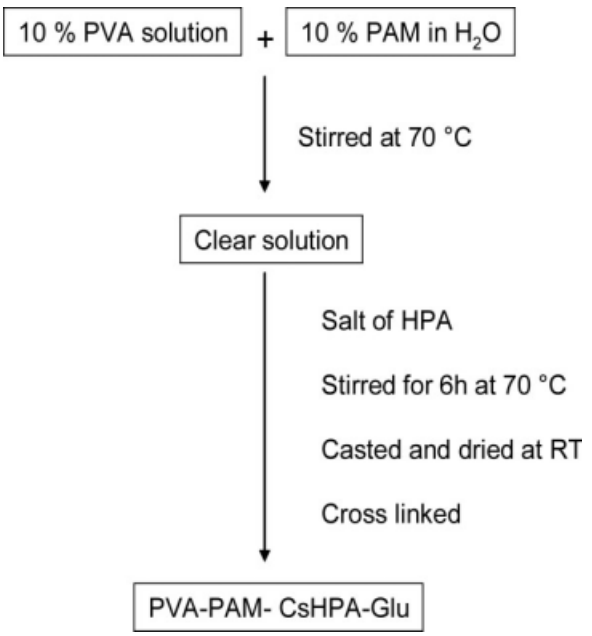

Scheme 1 Fabrication of hybrid membranes with different heteropolyacids (HPA).

voltage and amplitude of 5 mV.[22] Fully hydrated membranes were sandwiched in a Teflon conductivity cell equipped with Pt foil contacts, and we measured the impedance by placing the cell in a temperature-controlled chamber under the temperature range 303–353 K. Constant humidity was maintained at 50% relative humidity (RH) with saturated magnesium nitrate [$Mg(NO_3)_2$], and it was sensed by a hygrometer, which was calibrated before the experiments. The cyclic voltammetric technique (Bioanalytical Systems, West Lafayette, IN) was used to estimate the amount of crossed-over methanol, as described elsewhere.[23,35] Crossover studies were carried out at RT in this study. However, one has to remember that the methanol crossover in a real full cell system is influenced by operational conditions, such as cell temperature, thickness, and aging condition of the membrane, fuel concentration, and oxygen pressure. For this experiment, we used a two-compartment glass cell by mounting the membrane under examination at the middle by separating the two houses. These experiments were repeated three times to confirm the repeatability of the results obtained. The variation in the obtained results was found to be less than 2%.

Fabrication of the membrane electrode assembly (MEA)

The electrocatalysts used were unsupported Pt–Ru black (1 : 1 atomic ratio, Alfa Aesar, Ward Hill, MA) and Pt black (Alfa Aesar) in the anode and cathode, respectively. The catalyst slurry containing the catalyst, water, isopropyl alcohol, and Nafion solution (1100 EW, DuPont, Fayetteville, NC) as a binder was sprayed on a Teflonized carbon cloth (E-Tek, Somerset, NJ). Electrodes with 7 mg/cm^2 catalyst loadings were fabricated and placed on either side of the membrane. The MEA was sandwiched between the two transparent polyacrylic plates constituting the cell fixture by means of six bolts. The single-cell performance was measured with a passive DMFC with a 4*M* methanol solution. Methanol was diffused in the anode catalyst layer from the built-in reservoir, whereas oxygen, from the surrounding air, was diffused into the cathode catalyst layer through the opening of the cathode fixture. The single-cell performance experiments were carried out at RT and at atmospheric pressure. We measured cell voltage versus current density response by incrementally increasing the current from the open circuit and measuring the cell voltage.

RESULTS AND DISCUSSION

A new class of inorganic–organic hybrid membranes made through the blending of PVA and PAM followed by crosslinking with Glu. Cesium salts of different heteropolyacids, including PMA, PWA, and SWA, were incorporated into the polymer network to form corresponding hybrid membrane materials, namely, PVA–PAM–CsPMA–Glu, PVA–PAM–CsPWA–Glu, and PVA–PAM–CsSWA–Glu (where "Cs" together with a heteropolyacid abbreviation indicates the cesium salt of that acid), respectively, as described in the Experimental section. They were subjected to extensive physicochemical characterization studies.

FTIR spectral studies

Figure 1 shows the FTIR spectra of various hybrid membranes and their constituent materials from this study. As shown, the broad bands found in all three materials were attributed to the O—H stretching band for hydrogen-bonded alcohol at 3600 cm^{-1}. The bands at 1169 cm^{-1} were ascribed to (C—O) stretching, and the bands appearing at 1396 cm^{-1} were due to the C—O—H bending of PVA. The spectra exhibited a C—H alkyl stretching band at 2970 cm^{-1} and a C—H alkyl bending band at 1458 cm^{-1} for —CH_2 and —CH_3 bonds, respectively. The bands at 1746 and 2877 cm^{-1} indicated the aldehyde groups of Glu that was crosslinked to PVA. A weak band at 1671 cm^{-1} and a band at 1640 cm^{-1} were assigned to the —C=O stretching and N—H bending of the acrylamide unit in the hybrid polymer. The bands of the Keggin ion were observed between 1100 and 700 cm^{-1}.[36] The strong absorption band at about 1020 cm^{-1} in the hybrid membranes was

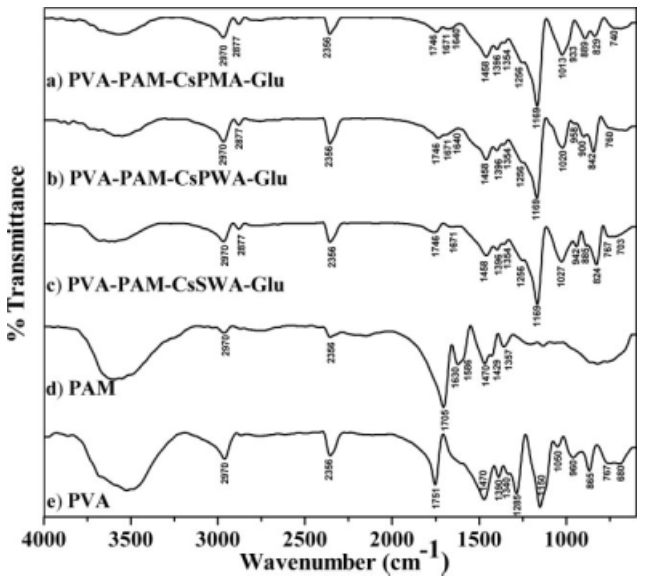

Figure 1 FTIR spectra of the hybrid membrane materials: PVA–PAM blends crosslinked by Glu with cesium salts of different heteropolyacids along with PAM and PVA.

assigned to the asymmetric stretching vibration of the central P—O_4 tetrahedron. The band at about 890 cm^{-1} was due to the stretching of M—O_c—M bridges between corner-sharing MO_6 octahedra, and that around 825 cm^{-1} was due to the stretching of M—O_e—M bridges between edge-sharing octahedra. The presence of these bands confirmed that the existence of the heteropolyacid with Keggin geometry was preserved in the hybrid membrane. The positions of the vibration modes of all types of metal–oxygen (M—O) bonds were strongly influenced by the interaction of the heteropolyacids with the polymer. The W—O_t (t = terminal) bond of SWA and PWA in the hybrid [Fig. 1(b,c)] was redshifted from 980 to 942 and 958 cm^{-1}, respectively. The stretching of the M—O_c—M bond with the corner-sharing oxygens of PMA, PWA, and SWA in the hybrid was blueshifted from 870 to 900, 890 to 900, and 878 to 884 cm^{-1}, respectively. This was due to the Coulombic interaction between the hydroxyl groups of the PVA and the heteropolyacid. The main bands are assigned and tabulated separately for the fabricated hybrid membranes in Table I.

X-ray diffraction (XRD) analysis

In Figure 2, the X-ray diffraction (XRD) profiles of the hybrid membranes incorporated with different heteropolyacids are shown. For a comparison, the XRD patterns of PVA and PAM are also given. The peak found at $2\theta = 20^\circ$ corresponded to the (1 0 1) plane of PVA in all of the hybrid membranes.[37] The broad diffraction pattern of PAM indicated the amorphous nature of the polymer. No diffraction peaks characteristic of CsSWA appeared in the hybrid membrane containing 10% SWA. This might have been due to the finely dispersed SWA in the polymer matrix, and the hybrid behaved as X-ray amorphous. Peaks characteristic of CsPMA and CsPWA appeared in the hybrid membranes containing the respective salts of the heteropolyacids. A broad peak in all of the hybrid membranes indicated the conformation of complete homogeneity and compatibility among the components of the membrane.

TGA studies

In Figure 3, the TGA traces of the hybrid membranes are shown in the temperature range from 40 to 800°C. The TGA curves of the hybrid membranes revealed four main weight-loss regions. The first weight loss was found in the region 100–200°C, and this was attributed to the loss of absorbed water molecules. The second weight loss, observed in the temperature region 200–425°C, was due to the

TABLE I
Assignments of the Main Absorption Bands of the Fabricated Hybrid Membranes

Vibration frequency (cm^{-1})			
PVA–PAM–CsPMA–Glu	PVA–PAM–CsPWA–Glu	PVA–PAM–CsSWA–Glu	Bond assignment
830	840	825	M—O_e—M stretching
900	900	885	M—O_c—M stretching
—	958	942	M—O_t stretching
	1027		X—O stretching
	1169		C—O stretching
	1256		C—O—C ether link
	1396		C—O—H bending
	1458		—CH_2 bending
	1640		N—H bending
	1671		Amide C=O stretching
	1746		Aldehyde C=O stretching
	2970		—CH_2 stretching
	3600		—OH stretching

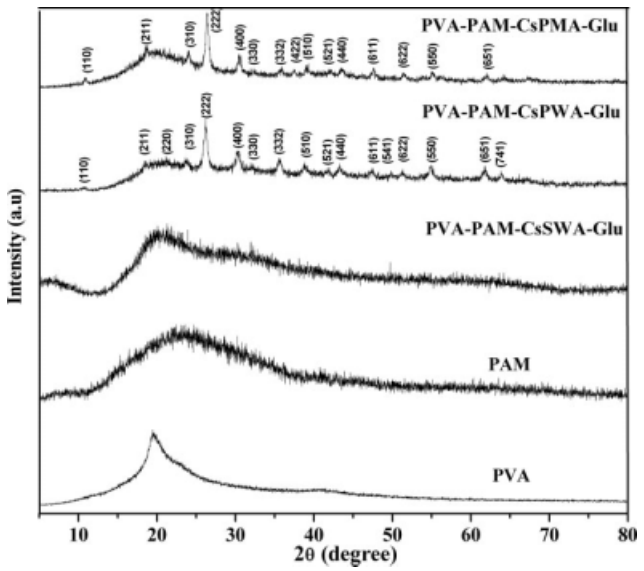

Figure 2 XRD patterns of the PVA–PAM hybrid membranes with different heteropolyacids.

degradation of PVA and PAM combined with the loss of crystalline water from the heteropolyacid. It was a complex decomposition process with thermal degradation of the ester and ether linkages formed during the process of crosslinking with gluteraldehyde. In addition, ammonia and water may have evolved partly from the polyacrylonitrile structure formed during the PAM decomposition and partly from the remaining PAM at about 400°C.[38] The third weight loss, found around 425–500°C, was ascribed to the cleavage of the C—C backbone of PVA and the PAM polymer membrane, which led to its carbonation. The fourth weight loss, at 550°C, was due to the decomposition of the salt of the heteropolyacid to its respective metal oxides. The three hybrid materials exhibited similar thermal behavior and showed that they had similar structural characteristics and were stable up to 200°C.

SEM interfaced with energy-dispersive X-ray analysis (EDXA)

The surface morphological characteristics of all three hybrid membranes in their dry state were examined with SEM. The SEM micrographs, along with corresponding EDXA spectroscopy traces, are shown in Figure 4. As shown in the micrographs, in all cases, the heteropolyacid particulates were finely dispersed in the polymer matrix. The distribution of inorganic particles appeared to be relatively uniform in the organic matrix. The average particle size of the heteropolyacid was around 50 nm. Furthermore, the presence of each of the heteropolyacid particles in the polymer matrix was elucidated from the corresponding peaks in the respective EDXA spectrographs.

Water uptake, swelling, and ion-exchange capacity (IEC)

After the physicochemical characterization and morphological studies, the three newly prepared hybrid materials were examined for their suitability to function as membrane materials for DMFCs. In this direction, the required key properties, including water uptake, swelling behavior, and IEC, of these materials were tested. The presence of water in the membrane greatly influenced the transport properties of these membranes. The water uptake and IEC played important roles in influencing the conductivity characteristics of the membranes. In Table II, the data obtained from the water uptake, swelling, and IEC studies of these materials are given. As shown, the extent of water uptake of the PMA-containing hybrid membrane was found to be higher (66%) compared to the other hybrid membranes with PWA (50%) and SWA (48%). The water uptake capacity of these studied hybrid membranes were twofold to threefold higher than that of the Nafion 115 membranes. At RT, the swelling extents of all of the fabricated hybrid membranes were found to be nearly fourfold to sixfold less than that of the commercial Nafion 115 membrane, although they maintained higher water uptakes because of the presence of hydrophilic properties of the heteropolyacid materials. A drastic decrease in the swelling extent of the fabricated PVA based hybrid membrane was attributed to the interpenetrating network that formed in the presence of PAM and Glu. The IECs of the hybrid membranes were slightly lower than that of the commercial Nafion 115 polymer electrolyte

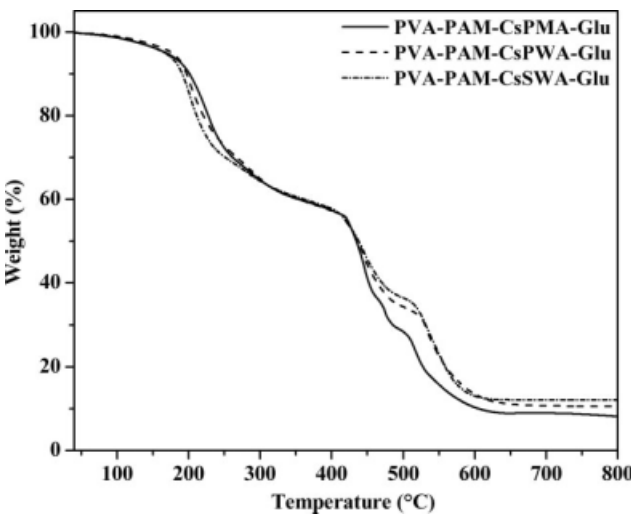

Figure 3 TGA traces of the hybrid membranes between 40 and 800°C.

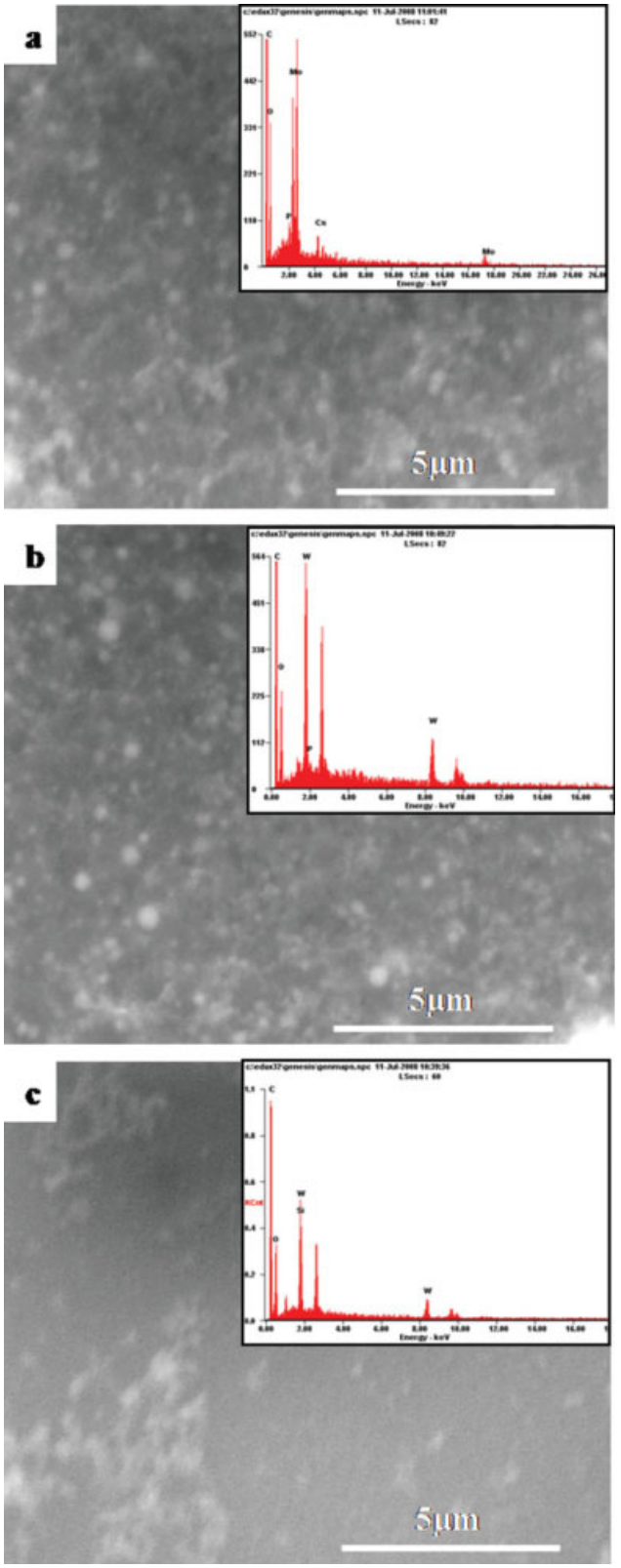

Figure 4 SEM micrographs of the surfaces of the hybrid membranes consisting of different heteropolyacids: (a) PVA–PAM–CsPMA–Glu, (b) PVA–PAM–CsPWA–Glu, and (c) PVA–PAM–CsSWA–Glu. The spectra represent the corresponding EDXA spectroscopy traces. [Color figure can be viewed in the online issue, which is available at www.interscience.wiley.com.]

membrane because of their inherent chemical compositions. Nafion holds the utmost electronegative environment possible in a chemical system.[2] The high electronegativity (i.e., electron affinity) of the fluorine atom, bonded to the same carbon atom to which the SO_3H group is present, makes the sulfonic acid a superacid (similar to trifluoromethane sulfonic acid). Hence, the proton in the perflurosulfonic acid moiety is more facile because of the inherent chemical composition of Nafion; this led to a significantly higher IEC than that of the newly fabricated composite membranes. Among the fabricated hybrid membranes, the CsPMA acid exhibited a higher IEC compared to the CsPWA and CsSWA acids containing hybrid membranes and, thus, affecting the proton conductivity.

Oxidative stability

The oxidative stability of the membrane material is of great concern because, under fuel cell operating conditions, the degradation of a polymer electrolyte is caused by the attack of HO· and HOO· radicals.[39] These radicals are formed because of the incomplete reduction of diffused oxygen at the anode. Hence, the oxidative stability of hybrid membranes was evaluated at RT in Fenton's reagent to simulate the fuel cell operating conditions. Figure 5 shows the results of the oxidative stability tests of the prepared hybrid membranes soaked in Fenton's reagent at RT. Oxidative stability testing carried out at RT indicated that all three fabricated hybrid membrane materials exhibited significantly higher stabilities. Initially, there was a steep increment in membrane weight, and the membrane attained a stable value and remained unchanged until 100 h. After 100 h, the weight of all three membranes decreased. Hence, the durability time of the hybrid membranes could be defined as the lasting time until the raising weight achieved a peak value,[40] and in these cases, it was 100 h. For comparison, pure PVA and PVA–PAM blends without heteropolyacids and with different blend densities were also studied. In 1 h, the pure PVA membrane completely dissolved at RT under oxidative treatment. PVA–PAM blends without heteropolyacids were stable until 2 h at RT, but they steadily lost their mechanical strength within that time. The improvement in oxidative stability of the hybrid membrane compared to its constituting components was due to its dense structure, which restricted the diffusion of the radicals into the membrane.

Additive stability

A critical problem associated with hybrid polymer electrolyte membranes is the leaching of the

TABLE II
Water Uptake, Swelling, and IEC Values for Different Hybrid Membranes Versus Nafion 115

Membrane	Thickness (μm)	Water uptake (%)	Swelling (%)	IEC (mequiv/g)
Nafion 115	125	22	12.0	0.90
PVA–PAM–CsPMA–Glu	250 ± 20	66	2.6	0.73
PVA–PAM–CsPWA–Glu	250 ± 20	50	2.0	0.67
PVA–PAM–CsSWA–Glu	250 ± 20	48	1.9	0.65

inorganic additive from the polymer matrix, which can lead to performance loss and/or system operational failures in a real fuel cell. Hence, to establish the stability of these membrane materials in this study, morphological characteristics of these membranes were tested at different time intervals for a duration of 5 days by the immersion of the membranes in water with the FTIR technique. Figure 6(a–c) shows the FTIR spectra of hybrid membranes containing various salts of heteropoly acids. Characteristic bands of Keggin ions were observed between 1100 and 700 cm^{-1}. All of the spectra confirmed the presence of a primary Keggin structure, which established the presence of the salts of the hereopolyacids in the hybrid membranes, even after they were immersed in water continually for several days. Initially, there was a decrease in the absorption intensity from 18 to 73 h of immersion. After 73 h, the decrease became negligible. This showed that the salts of the heteropolyacids present on the surface were washed out in the initial stage because of the vigorous stirring conditions, whereas the salts of the heteropolyacids presented well inside the three-dimensional network of the polymer matrix were quite stable. These spectra remained similar, even after 125 h; this represented a negligible amount of loss in the salts of the heteropolyacid because of the vigorous stirring conditions. These results ascertain the stability of the Cs salts of the heteropolyacids in the PVA–PAM matrices.

Proton conductivity study

Figure 7 shows the proton conductivity characteristics of the fabricated hybrid membranes measured at various temperatures ranging from 30 to 90°C and at 50% RH. For comparison, the proton conductivity of the commercial Nafion 115 polymer electrolyte membrane measured at 100% RH is shown. The presence of the salt of the heteropolyacid and the highly acidic N—H proton of PAM with a hydrogen-bonded interpenetrating network of the polymer matrix led to facile proton transport through the membrane under low humidity.

Among the hybrid membranes studied, CsPMA-substituted hybrid membranes exhibited a higher conductivity compared to the CsPWA- and CsSWA-substituted systems. The order of proton conductivities of the hybrid membranes was in accordance with the water uptake ability and IEC of the materials (Table II). The proton conductivity depended on the water uptake; this implied the effect of the water channels or domains formed in the polymer matrix for facilitating proton transport inside the hybrid matrix. The proton conductivity of the hybrid membranes increased with increasing water content.

In particular, the PVA–PAM–CsPMA–Glu membrane exhibited the highest proton conductivity in the range 10^{-2} S/cm at 50% RH. The superior proton conductivity attained in the CsPMA-containing system was attributed to the more ionic nature of the Mo—O_t bond compared to the W—O_t bonds. This ionic character imparted a protonic character to the hydrogen on these sites. Because the W—O bond was more covalent, the protons were not free as in the case with the Mo—O system. In addition, the presence of cesium ions made the system more polarizable. The charge on the heteropoly anion was spread, and the size of the anion [$PMo_{12}O_{40}^{3-}$ (5.4 Å) < $PW_{12}O_{40}^{3-}$ (5.6 Å)] was yet another factor. It was not the net charge on the M—O (metal–oxygen) terminal bond alone that contributed to the proton conductivity.

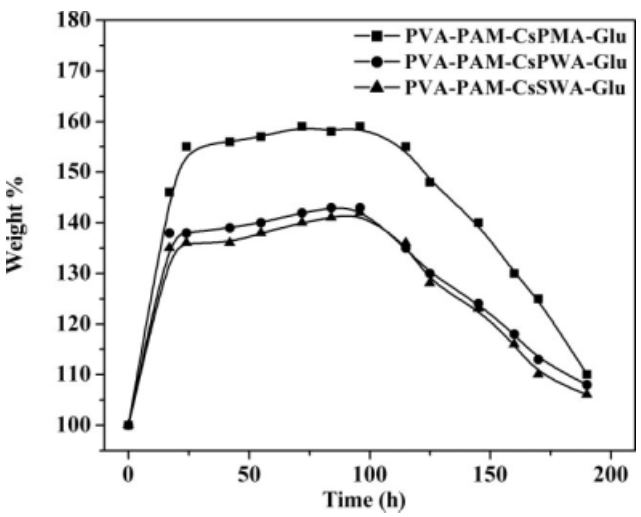

Figure 5 Oxidative stability of the fabricated membranes immersed at RT in Fenton's reagent at various time intervals.

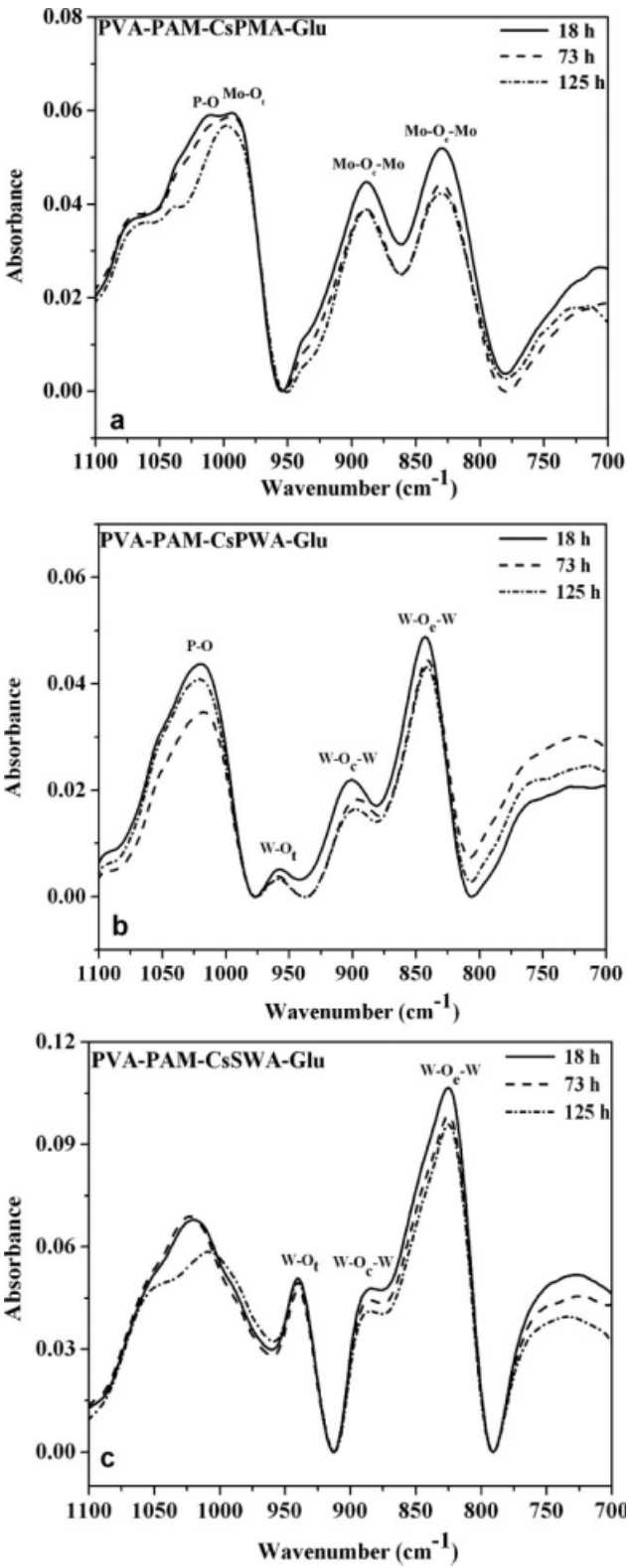

Figure 6 FTIR spectra of the hybrid membranes placed in water for different durations: (a) PVA–PAM–CsPMA–Glu, (b) PVA–PAM–CsPWA–Glu, and (c) PVA–PAM–CsSWA–Glu.

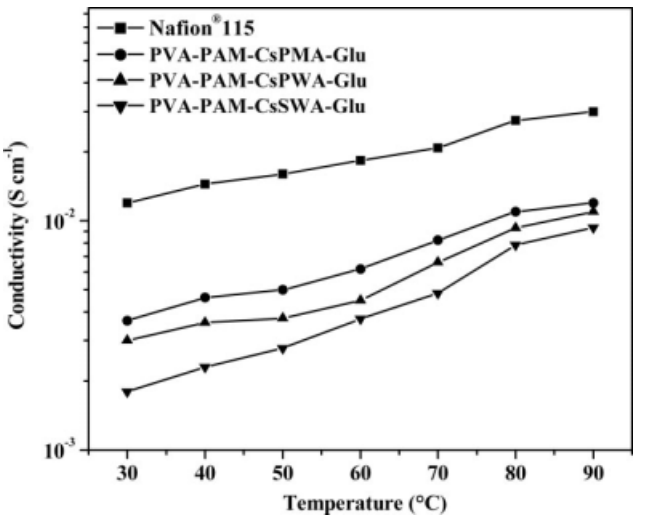

Figure 7 Proton conductivity of the fabricated hybrid membranes and Nafion 115 membrane at different temperatures.

Also, the proton conductivities of the fabricated hybrid membranes were less than that of the state-of-the-art Nafion 115 membrane. Perfluorosulfonate proton-exchange membranes, such as Nafion membrane materials, enjoy the status of premium proton conductivity among all membrane materials because of their inherent chemical composition.

Methanol crossover study

The concentration of permeated methanol through the hybrid membrane materials, including PVA–PAM–CsPMA–Glu, PVA–PAM–CsPWA–Glu, and PVA–PAM–CsSWA–Glu, as a function of crossover time was measured with the cyclic voltammetric technique and with a two-compartment cell, which we divided by housing corresponding membrane

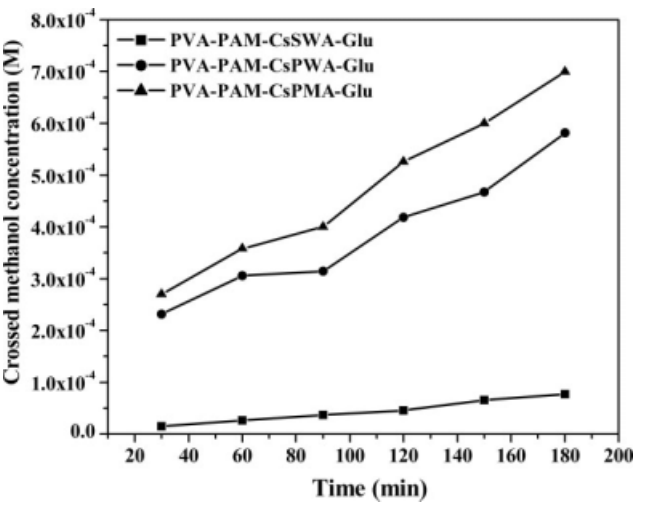

Figure 8 Concentration of crossed-over methanol as a function of the crossover time.

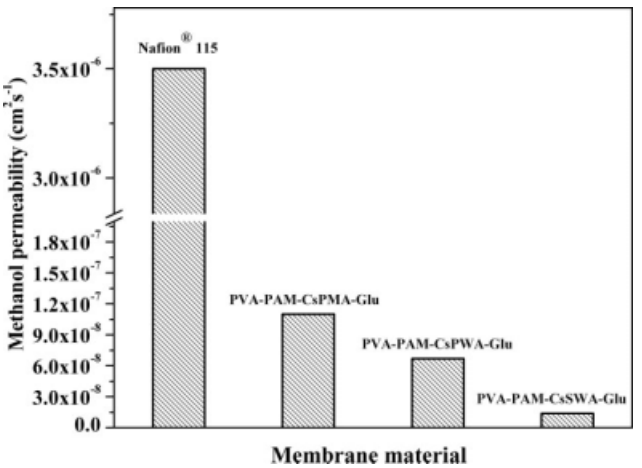

Figure 9 Methanol permeability results for the fabricated hybrid membranes versus Nafion 115.

materials. The results of methanol crossover studies are presented in Figure 8. The rate of crossed over methanol appeared to vary with the variation in incorporated heteropolyacid material. The hybrid membrane containing SWA as an active component exhibited a lower rate of methanol crossover compared to the other heteropolyacid materials, including the PWA- or PMA-containing hybrid membranes. The concentration of crossed methanol through the PVA–PAM–CsSWA–Glu hybrid membranes after 180 min was threefold less than that through PVA–PAM–CsPWA–Glu and four times lower than through the PVA–PAM–CsPMA–Glu system. The methanol permeability of the respective membranes was determined from the slope of the plots representing the crossed methanol concentration versus time (Fig. 8). Figure 9 shows the quantitative representation of the methanol permeability of the hybrid membranes, and the results were compared with that of commercial Nafion 115 membrane. The methanol permeability was an order of magnitude lower for the fabricated hybrid membranes compared to Nafion 115. This may have been due to the dense interpenetrating network that was formed because of the blending of PVA with PAM followed by crosslinking with Glu.

The increasing order of methanol permeabilities of the membrane materials can be given as PVA–PAM–CsSWA–Glu < PVA–PAM–CsPWA–Glu < PVA–PAM–CsPMA–Glu ≪ Nafion 115 (Fig. 9). The reduced methanol permeation in the hybrid membranes compared with Nafion 115 was considered an attractive desirable characteristic for scientists and engineers working in the DMFC field, and this property was attributed to the methanol absorption ability of the heteropolyacids that were incorporated into the polymer matrix of the PVA–PAM blend. Because of the flexible nature of the secondary structure, heteropolyacids possess a unique conceptual character called *pseudoliquid phase behavior*, in which polar molecules such as methanol can be readily absorbed into the solid matrix.[41] The water molecules in the secondary structure of the heteropolyacids were substituted by the methanol molecules. Hence, the fabricated heteropolyacid containing hybrid membranes exhibited the capacity to retain methanol without letting it pass by. The number of methanol molecules adsorbed per anion is approximated by the integral number of protons in the heteropoly molecule.[42–44] The order of methanol adsorption per Keggin unit was reported to be as follows: $SiW_{12}O_{40}^{4-} > PW_{12}O_{40}^{3-} > PMo_{12}O_{40}^{3-}$,[42,44–47] which was clearly reflected in our results of the

TABLE III
Comparison of the Proton Conductivity and Methanol Permeability of Various Membranes

Membrane materials	RH (%)	Temperature (°C)	Conductivity (S/cm)	Permeability (cm^2/s)	Reference
PVA–PAM–CsSWA–Glu	50	RT	1.8×10^{-3}	1.38×10^{-8}	This study
PVA–PAM–CsPWA–Glu	50	RT	3×10^{-3}	6.7×10^{-8}	This study
PVA–PAM–CsPMA–Glu	50	RT	3.7×10^{-3}	1.1×10^{-7}	This study
PVA–ZrP–SWA	60	60	10^{-2}	6×10^{-7}	23
PVA–ZrP–Cs_1SWA	50	100	0.013	2×10^{-6}	22
PVA–ZrP–Cs_2SWA	50	100	0.02	3×10^{-6}	22
PVA/PWA/SiO_2	—	—	0.004–0.017	10^{-7} to 10^{-8}	26
PVACO/PMA	—	30–100	10^{-3}	10^{-6}	29
PEG/SiO_2/SWA	100	80	0.01	10^{-5} to10^{-6}	30
PEG/SiO_2/PWA	—	—	10^{-5} to 10^{-3}	10^{-6} to10^{-7}	31
SPEEK/PWA	100	100	1.7×10^{-2}	—	32
SPEEK/TPA/MCM-41	—	20	2.75×10^{-3}	10^{-8}	33
Nafion 115	100	90	0.03	3.5×10^{-6}	22
CRA-08	—	60	45×10^{-3}	0.58×10^{-6}	47 and 48
IonClad R1010	—	60	146×10^{-3}	0.6×10^{-6}	49 and 50
SPEEK[a]	—	60	13×10^{-3}	17.5×10^{-7}	51–53

[a] Sulfonation degree = 87%. The subscript in Cs_1SWA and Cs_2SWA in the first column represent the number of protons substituted by Cs in the silicotungstic acid, i.e., Cs_1SWA for $Cs_1H_3SiW_{12}O_{40}$ and Cs_2SWA for $Cs_2H_2SiW_{12}O_{40}$.

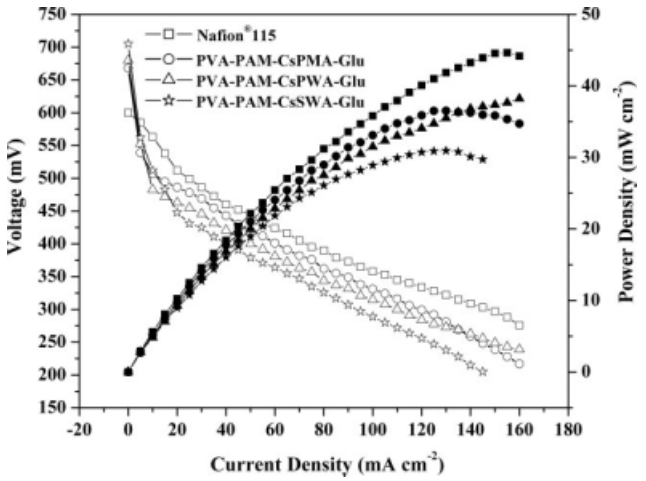

Figure 10 Polarization and power-density curves of the passive DMFC with the fabricated hybrid membranes and Nafion 115 at RT and at atmospheric pressure.

permeability studies. Thus, a reduced methanol permeability was observed for the hybrid membrane with CsSWA (PVA–PAM–CsSWA–Glu = 1.38×10^{-8} cm^2/s) compared to other the heteropolyacid-containing hybrid membranes. Compared to the Nafion 115 membrane, other commercial membranes, and related hybrid membranes, the fabricated hybrid membranes in this study exhibited excellent tolerance to methanol permeability with appreciable proton conductivity, as shown by the values given in Table III.

Single-cell performance in DMFC

The single cell performance of DMFCs with three fabricated hybrid membranes along with Nafion 115 is shown in Figure 10. The voltage–current density curves for the fabricated hybrid membranes was below that of the reference membrane Nafion 115. The slight decrease in the cell performance of the fabricated hybrid membranes was due to the membrane thickness (250 μm) and the lower proton conductivity compared to Nafion 115. Among the fabricated hybrid membranes, the MEA made of PVA–PAM–CsPMA–Glu exhibited a higher performance than the MEAs made of PVA–PAM–CsPWA–Glu and PVA–PAM–CsSWA–Glu hybrid membranes. A power density of 37 mW/cm at a load current density of 125 mA/cm^2 was observed for the MEA made of PVA–PAM–CsPMA–Glu; this was higher than power densities for the MEAs fabricated with PVA–PAM–CsPWA–Glu (35 mW/cm^2) and PVA–PAM–CsSWA–Glu (31 mW/cm^2) hybrid membranes. The improved performance of the former membrane was due to the improved proton conductivity. Among the fabricated hybrid membranes with different salts of heteropolyacids, the order of single-cell performance was in accordance with the conductivity of the membranes. The fabricated hybrid membranes with reduced thicknesses are expected to result in performances comparable to that of Nafion 115. Efforts are underway to make thinner hybrid membrane materials.

The open-circuit voltages (OCVs) for the air-breathing passive cells with PVA–PAM–CsPMA–Glu, PVA–PAM–CsPWA–Glu, and PVA–PAM–CsSWA–Glu hybrid membranes were 0.668, 0.680, and 0.705 V, respectively. The relatively high OCV values observed for all of the hybrid membranes were an indication of a significantly lower methanol crossover to the cathode side compared to that in the Nafion 115 (0.602 V) membrane. These results indicate that the fabricated hybrid membranes are suitable candidates for DMFC applications.

CONCLUSIONS

In conclusion, we successfully formulated, fabricated, and demonstrated the formation of PVA-based hybrid membranes with key properties desired for DMFC applications, such as low methanol crossover, low swelling, good oxidation stability, and appreciable proton conductivity for the first time. The interpenetrating network formed by the blending of PVA with PAM led to an order of decrease in methanol crossover and swelling compared to the state-of-the-art Nafion 115 membrane used for DMFC applications. The difference in methanol permeability between the fabricated hybrid membranes containing different cesium salts of heteropolyacids was found to be governed by the adsorption ability of the respective heteropolyacids. The enhanced IEC and reasonable water uptake characteristics endowed the studied hybrid membrane materials with appreciable proton conductivities. Morphological evidence from SEM interfaced with EDXA showed an even distribution of salts of the heteropolyacids throughout the polymer matrix. The relatively high OCV (0.66 V) observed for all hybrid membranes was indicative of a significantly lower methanol crossover to the cathode side compared to that in the Nafion 115 (0.602 V) membrane. These preliminary results unequivocally prove the potential capacities of the PVA–PAM-based hybrid membranes with cesium salts of heteropolyacids as an electrolyte material for DMFC applications because of their reduced methanol crossover property, which is considered a major drawback for expensive, fluorine-based commercial Nafion 115 membranes.

The authors thank the Department of Science and Technology for the support to the National Centre for Catalysis Research. The Council of Scientific and Industrial Research, India, is gratefully acknowledged for a Senior Research Fellowship to one of the authors (M.H).

References

1. Surampudi, S.; Narayanan, S. R.; Vamos, E.; Frank, H.; Halpert, G.; LaConti, A.; Kosek, J.; Surya Prakash, G. K.; Olah, G. A. J Power Sources 1994, 47, 377.
2. Viswanathan, B.; Helen, M. Bull Catal Soc India 2007, 6, 50.
3. Alberti, G.; Casciola, M. Annu Rev Mater Res 2003, 33, 129.
4. Nunes, S. P.; Ruffmann, B.; Rikowski, E.; Vetter, S.; Richau, K. J Membr Sci 2002, 203, 215.
5. Cho, K.-Y.; Jung, H.-Y; Shin, S.-S.; Choi, N.-S.; Sung, S.-J.; Park, J.-K.; Choi, J.-H.; Park, K. W.; Sung, Y.-E. Electrochim Acta 2004, 50, 588.
6. Qiao, J. L.; Hamaya, T.; Okada, T. J Mater Chem 2005, 15, 4414.
7. Nagarale, R. K.; Gohil, G. S.; Shahi, V. K.; Rangarajan, R. J Membr Sci 2006, 280, 389.
8. Zhonga, S.; Cui, X.; Cai, H.; Fua, T.; Shao, K.; Naa, H. J Power Sources 2007, 168, 154.
9. Matsuguchi, M.; Takahashi, H. J Membr Sci 2006, 281, 707.
10. Jia, N.; Lefebvre, M. C.; Halfyard, J.; Qi, Z.; Pickup, P. G. Electrochem Solid State Lett 2000, 3, 529.
11. Kim, J.; Kim, B.; Jung, B. J Membr Sci 2002, 207, 129.
12. Won, J.; Park, H. H.; Kim, Y. J.; Choi, S. W.; Ha, H. Y.; Oh, I. H.; Kim, H. S.; Kang, Y. S.; Ihn, K. J. Macromolecules 2003, 36, 3228.
13. Elabd, Y. A.; Walker, C. W.; Beyer, F. L. J Membr Sci 2004, 231, 181.
14. Walker, M.; Baumgärtner, K.-M.; Feichtinger, J.; Kaiser, M.; Räuchle, E.; Kerres, J. Surf Coat Technol 1999, 116, 996.
15. Choi, W. C.; Kim, J. D.; Woo, S. I. J Power Sources 2001, 96, 411.
16. Hobson, L. J.; Ozu, H.; Yamaguchi, M.; Hayase, S. J Electrochem Soc A 2001, 148, 1185.
17. Bae, B.; Chun, B.-H.; Ha, H.-Y.; Oh, I.-H.; Kim, D. J Membr Sci 2002, 202, 245.
18. Dimitrova, P.; Friedrich, K. A.; Vogt, B.; Stimming, U. J Electroanal Chem 2002, 532, 75.
19. Shen, J.; Xi, J.; Zhu, W.; Chen, L.; Qiu, X. J Power Sources 2006, 159, 894.
20. Aricò, A. S.; Cretì, P.; Antonucci, P. L.; Antonucci, V. Solid State Lett 1998, 1, 66.
21. Libby, B.; Smyrl, W. H.; Cussler, E. L. AIChE J 2003, 49, 991.
22. Helen, M.; Viswanathan, B.; Srinivasa Murthy, S. J Power Sources 2006, 163, 433.
23. Helen, M.; Viswanathan, B.; Srinivasa Murthy, S. J Membr Sci 2007, 292, 98.
24. Pivovar, S. B.; Wang, Y.; Cussler, E. L. J Membr Sci 1999, 154, 155.
25. Polak, A. J.; Weeks, S. P.; Beuhler, A. J. Sens Actuators 1986, 9, 1.
26. Xu, W.; Liu, C.; Xue, X.; Su, Y.; Lv, Y.; Xing, W.; Lu, T. Solid State Ionics 2004, 171, 121.
27. Qiao, J.; Hamaya, T.; Okada, T. Chem Mater 2005, 17, 2413.
28. Lin, C. W.; Huang, Y. F.; Kannan, A. M. J Power Sources 2007, 171, 340.
29. Arfat, A.; Banthia, A. K.; Bandyopadhyay, S. J Power Sources 2008, 179, 69.
30. Vernon, D. R.; Meng, F.; Dec, S. F.; Williamson, D. L.; Turner, J. A.; Herring, A. M. J Power Sources 2005, 139, 141.
31. Lin, C. W.; Thangamuthu, R.; Chang, P. H. J Membr Sci 2005, 254, 197.
32. Ponce, M. L.; Prado, L.; Ruffmann, B.; Richau, K.; Mohr, R.; Nunes, S. P. J Membr Sci 2003, 217, 5.
33. Bello, M.; Zaidi, S. M. J.; Rahman, S. U. J Membr Sci 2008, 322, 218.
34. Ramani, V.; Kunz, H. R.; Fenton, J. M. J Membr Sci 2004, 232, 31.
35. Ling, J.; Savadogo, O. J Electrochem Soc A 2004, 151, 1604.
36. Deltcheff, C. R.; Thouvenot, R.; Franck, R. Spectrochim Acta 1976, 32, 587.
37. Koji, N.; Tomonori, Y.; Kenji, I.; Fumio, S. J Appl Polym Sci 1999, 74, 133.
38. Tutas, M.; Saglam, M.; Yuksel, M.; Guler, C. Thermochim Acta 1987, 111, 121.
39. Hübner, G.; Roduner, E. J Mater Chem 1999, 9, 409.
40. Fu, R.-Q.; Woo, J.-J.; Seo, S.-J.; Lee, J.-S.; Moon, S.-H. J Power Sources 2008, 179, 458.
41. Misono, M. Catal Rev Sci Eng 1987, 29, 269.
42. Okuhara, T.; Tatematsu, S.; Lee, K. Y.; Misono, M. Bull Chem Soc Jpn 1989, 62, 717.
43. Bielanski, A.; Datka, J.; Gil, B.; Lubanska, A. M.; Ilnicka, A. M. Phys Chem Chem Phys 1999, 1, 2355.
44. Małecka, A.; Pózniczek, J.; Ilnicka, A. M.; Bielánski, A. J Mol Catal A Chem 1999, 138, 67.
45. Bielánski, A.; Lubnska, A.; Ilnicka; A. M.; Pózniczek, J. Coord Chem Rev 2005, 249, 2222.
46. Rykova, A. I.; Burkat, T. M.; Pak, V. N. Russ J Gen Chem 2003, 73, 697.
47. Antonucci, V.; Aricò, A. S.; Baglio, V.; Brunea, J.; Buder, I.; Cabello, N.; Hogarth, M.; Martin, R.; Nunes, S. Desalination 2006, 200, 653.
48. Amara, M.; Kerdjoudj, H. Desalination 2003, 155, 79.
49. Scott, K.; Taama, W. M.; Argyropoulos, P. J Membr Sci 2000, 171, 119.
50. Tricoli, V.; Carretta, N.; Bartolozzi, M. J Electrochem Soc 2000, 147, 1286.
51. Li, L.; Zhang, J.; Wang, Y. J Mater Sci Lett 2003, 22, 1595.
52. Silva, V. S.; Ruffmann, B.; Silva, H.; Silva, V. B.; Mendes, A.; Madeira, L. M.; Nunes, S. J Membr Sci 2006, 284, 137.
53. Fu, T.; Zhao, C.; Zhong, S.; Zhang, G.; Shao, K.; Zhang, H.; Wang, J.; Na, H. J Power Sources 2007, 165, 708.